Half the story: thermal effects on within-host infectious disease progression in a warming climate

Running head: Immunity in a warming climate

ALEXANDER STEWART[1], PASCAL I. HABLÜTZEL[2,3,4], MARTHA BROWN[2], HAYLEY V. WATSON[2,5], SOPHIE PARKER-NORMAN[2], ANYA V. TOBER[1], ANNA G. THOMASON[6], IDA M. FRIBERG[6], JOANNE CABLE[1§], JOSEPH A. JACKSON[6§*]

[1] *School of Biosciences, Cardiff University, Cardiff CF10 3AX, UK*

[2] *IBERS, Aberystwyth University, Aberystwyth SY23 3DA, UK*

[3] *Flanders Marine Institute, Oostende 8400, Belgium*

[4] *Laboratory of Biodiversity and Evolutionary Genomics, Biology Department, University of Leuven, 3000 Leuven, Belgium*

[5] *School of Environmental Sciences, University of Hull, Hull, HU6 7RX, UK*

[6] *School of Environment and Life Sciences, University of Salford, Salford M5 4WT, UK*

§ JC and JAJ are joint senior authors.

*Corresponding author: J.A.Jackson@Salford.ac.uk; tel. +44 161 2952240.

Keywords: Infection, immunity, ectothermic, vertebrate, *Gasterosteus aculeatus*, teleost, parasite, disease, phenology, systems analysis.

PRIMARY RESEARCH ARTICLE

Abstract

Immune defence is temperature-dependent in cold-blooded vertebrates (CBVs) and thus directly impacted by global warming. We asked whether immunity and within-host infectious disease progression are altered in CBVs under realistic climate warming in a seasonal mid-latitude setting. Going further, we also asked how large thermal effects are in relation to the effects of other environmental variation in such a setting (critical to our ability to project infectious disease dynamics from thermal relationships alone). We employed the three-spined stickleback and three ecologically-relevant parasite infections as a “wild” model. To generate a realistic climatic warming scenario we used naturalistic outdoors mesocosms with precise temperature control. We also conducted laboratory experiments to estimate thermal effects on immunity and within-host infectious disease progression under controlled conditions. As experimental readouts we measured disease progression for the parasites and expression in 14 immune-associated genes (providing insight into immunophenotypic responses). Our mesocosm experiment demonstrated significant perturbation due to modest warming (+2°C), altering the magnitude and phenology of disease. Our laboratory experiments demonstrated substantial thermal effects. Prevailing thermal effects were more important than lagged thermal effects and disease progression increased or decreased in severity with increasing temperature in an infection-specific way. Combining laboratory-determined thermal effects with our mesocosm data, we used inverse modelling to partition seasonal variation in *Saprolegnia* disease progression into a thermal effect and a latent immunocompetence effect (driven by non-thermal environmental variation and correlating with immune gene expression). The immunocompetence effect was large, accounting for at least as much variation in *Saprolegnia* disease as the thermal effect. This suggests that managers of CBV populations in variable environments may not be able to reliably project infectious disease risk from thermal data alone. Nevertheless, such projections would be improved by primarily considering prevailing (not lagged) temperature variation and by incorporating validated measures of individual immunocompetence.

Introduction

During infection, host immunity constrains the effectiveness with which a parasite exploits its host, determining disease outcome. In cold-blooded animals this within-host tension is modulated by environmental temperature, as both host immunity and parasite development are thermally dependent (Jackson & Tinsley, 2002; Garner *et al.*, 2011), each with a given thermal reaction norm (Scheiner, 1993). Where these reaction norms do not perfectly offset each other (Jackson & Tinsley, 2002), temperature changes, such as those generated during global warming, may shift susceptibility and disease progression within hosts. In turn, this may contribute to the wider dynamics of disease through changing the production rate of propagules (in definitive hosts) or the within-host survival of larval stages (in intermediate hosts). In natural environments, the size of thermal effects, and how these measure against the effects of non-thermal environmental variation (including variation driven indirectly by temperature regimen), is very poorly understood. Thus, it is equally poorly understood whether incremental warming would affect infectious disease systems mostly directly through thermal effects or indirectly through temperature-driven environmental variation. This dichotomy is key to our ability to project infectious disease dynamics on the basis of thermal relationships alone.

Given the above uncertainties, we set out to measure thermal effects on immunity and infectious disease progression in a cold-blooded vertebrate (CBV) model and to place these effects within the context of other natural environmental effects. We specifically focussed on within-host processes (excluding extra-host processes contributing to transmission) and considered a seasonal mid-latitude study system, which allowed the analytically powerful approach of using sinusoid functions to disentangle the contributions of distinct seasonally variable drivers. We created a realistic warming scenario, where we superimposed a thermal increment upon natural year-round environmental cycles, and observed the resulting variation. This allowed us to measure the perturbation caused by warming; but, critically, by itself did not allow us to quantify the separate thermal and non-thermal processes determining the observed outcomes. Crucially, we took the important further step of combining infection and thermal measurements from the realistic scenario with estimates from laboratory experiments where we had characterized thermal effects

precisely under controlled conditions. Taking a systems (inverse modelling) approach we were then able to use sinusoid functions to analytically decompose the relative contributions of thermal and non-thermal environmental effects.

We employed the mid-latitude three-spined stickleback (*Gasterosteus aculeatus*) and its pathogens as a natural cold-blooded vertebrate (CBV) model. We kept in mind that, in variable temperature regimens in natural habitats, past thermal variation may feed forwards effects on physiological responses (Jackson & Tinsley, 2002; Podrabsky & Somero, 2004; Raffel *et al.*, 2006, 2013, 2015; Garner *et al.*, 2011; Murdock *et al.*, 2012; Dittmar *et al.*, 2014; Altman *et al.*, 2016). Our laboratory experiments below therefore incorporated thermal change, allowing us to assess the importance of both prevailing and time-lagged thermal effects on infectious disease progression under natural seasonal thermal variation.

As phenotypic readouts we directly measured infection outcomes (Viney *et al.*, 2005) in three ecologically-relevant infection systems with differing modes of established infection. The directly-transmitted oomycete *Saprolegnia parasitica* (see Jiang *et al.*, 2013) produces a rapidly proliferating mould-like infection following initial colonization by spores. Once established, these infections cause acute disease, often overwhelming small fish hosts within hours or a few days post-infection. The life history of the gyrodactylid monogenean *Gyrodactylus gasterostei* (see Harris, 1982), in contrast, is based on precocious (born near full size), directly-transmitted viviparous flukes. A specialised larval transmission stage is absent: suprapopulations persisting through *in situ* proliferation on individual hosts and the migration of individuals from host to host. Gyrodactylid infections cause significant disease on small fish that, if not fatal, may be self-limiting over a time scale of weeks or months. In the cestode *Schistocephalus solidus* (see Barber & Scharsack, 2010) the stickleback is the second intermediate host in an indirect life cycle, becoming infected through the ingestion of copepod first intermediates. The non-proliferating *S. solidus* plerocercoid larva may grow to great relative size (up to 50% of host weight, or more), causing significant chronic disease and deformity over months or even years. Our measurements for the respective infection systems (body surface coverage by mycelia in *Saprolegnia*, abundance in *Gyrodactylus*, plerocercoid weight in *Schistocephalus*) are in each case clear surrogates for disease

severity (Roberts, 2012). To provide insight into thermal effects on immunocompetence we also measured (mRNA) expression for 14 immune-associated genes representing different pathways (Hablützel *et al.*, 2016).

We quantified thermal effects under controlled conditions in two separate laboratory experimental designs. These employed relatively large (but ecologically relevant) temperature variations in order to increase the precision of estimated effects (i.e., maximizing the signal to noise ratio). One experiment examined the effects of constant temperatures and of short-term temperature change, and the other the effects of long-term cold exposures followed by periods of rising temperature (simulating spring-like warming following winter). To generate the realistic warming scenario mentioned above we conducted an outdoors mesocosm experiment using an array of semi-natural tank habitats. We monitored phenotypes monthly, for a year (from one autumn to the next), in a cohort of initially post-larval fish maintained in the mesocosm tanks. The design was repeated twice, in separate successive years with different fish cohorts. Half of the tanks were unheated and exposed to natural temperature variation, whilst the other half were heated (precisely, using immersion heaters with differential thermostatic control) to 2°C above the temperature of the unheated tanks. This increment represents a large, but not unrealistic, stochastic variation in mean temperature between successive years (O'Reilly *et al.*, 2015; Sharma *et al.*, 2015) in temperate zone aquatic habitats. Such increases would be expected to be more common, if as the Intergovernmental Panel on Climate Change (IPCC) predicts, there is up to a 4.8°C rise in global mean surface temperature by 2100 (IPCC, 2014).

Our study aimed to represent processes in the field as far as possible whilst, at the same time, exerting sufficient experimental control. Although, natural temperature and photoperiod aside, tanks in our mesocosm experiment were not a fully natural environment, they did undergo naturalistic cycles. Thus, seasonally variable planktonic assemblages formed within the mesocosms and stickleback underwent seasonal patterns of immune gene expression (Brown *et al.*, 2016), albeit that these patterns were diminished from those seen in the wild (Hablützel *et al.*, 2016). Furthermore, all of our experiments utilized quarantined anti-parasite treated wild fish that had been acclimatized to laboratory or mesocosm conditions. In this choice of

hosts we aimed for subjects with as natural a phenotype as possible, but lacking directly-transmitted pathogens capable of producing epidemics that might confound the experimental structure. This approach was important given the likelihood that laboratory-raised animals would have phenotypes very unrepresentative of the wild (Robertson *et al.*, 2016).

Below we thus ask whether immunity and infectious disease progression in a model naturally-occurring CBV are detectably perturbed in a realistic, seasonal, climate warming scenario. We measure the size of thermal influences in the laboratory and ask whether these are mediated by prevailing and lagged effects. Finally, combining the different elements of our study (as outlined above), we partition thermal effects on disease progression from effects due to other temporal environmental variation and ask whether thermal effects are dominant in a natural seasonal environment.

Materials and methods

Terminology

For gene expression, we define prevailing thermal effects as those due to temperature around the time of measurement and lagged effects as those due to temperature at some interval before the time of measurement. For infections, prevailing and lagged temperature effects are defined in relation to the timing of parasite invasion. Prevailing thermal effects are those due to temperature within the timeframe of infection. Lagged thermal effects are those due to temperature prior to infection.

Experimental designs and methods

Overview. We carried out two laboratory experiments to characterize thermal effects on infection and immunity under controlled conditions. Both of these featured factorial combinations of prevailing and lagged temperature treatments. In the first experiment (experiment 1) we subjected fish to different constant temperatures and then to short-term temperature shifts. In the second (experiment 2) we subjected fish to differing long-term cold temperature regimens (simulating winters of different length) followed by synchronized convergence on a warmer temperature (simulating

spring-like warming). In a third experiment (experiment 3), to simulate climate warming in a naturalistic seasonal environment, we maintained fish year-round in semi-natural outdoor mesocosms, superimposing a small thermal increment upon natural thermal variation. The structure of these experiments (involving experimental manipulations of >1500 fish) is summarised in Fig. 1 and described in detail below and in Supplementary appendix S1.

Experiment 1 (prevailing temperature vs short-term lagged effects in the laboratory). Wild *G. aculeatus* captured at Roath Brook, Cardiff, Wales, U.K. (RBK; 51.4998°, -3.1688°) in October 2014 and 2015 were transferred to the aquarium facility at Cardiff University. Here they were quarantined at a density of <1 individual L^{-1} in 30 L fresh water tanks at 15±0.5°C with 18L:6D photoperiod. All individuals were treated for parasites using adaptations of treatments listed by Shinn & Bron (2012). Initially fish were subjected to submersion in 0.004% formaldehyde solution for a total of 1 h over a 1.5 h period (30 min exposure: 30 min rest in freshwater: 30 min exposure). Following a further 24 h in fresh water, fish were then treated with praziquantel (Vetark) according to the manufacturer's instructions (4 mg L^{-1} for 48 h). Following this treatment, fish were maintained for 1 week in 1% aquarium salt solution and 0.002 g L^{-1} methylene blue to prevent secondary bacterial or fungal infection and manually cleared of any remaining gyrodactylid infections following Schelkle *et al.* (2009). Uninfected fish were then returned to fresh water (in 30L tanks, as above) and acclimatised to laboratory conditions for a further one month quarantine period (during which they were monitored for overt infections). Acclimatized fish were weighed and measured (standardized body length, mm; body weight, mg) and randomly allocated to 3 different groups (Fig. 1) that were respectively maintained at 7, 15 or 23°C for 3 weeks. Temperature treatment groups were then further sub-divided (randomly) into temperature shift treatment groups. For the next 6 h these temperature shift treatment groups were either maintained at the same temperature as before (constant temperature groups), or shifted between temperatures (7 to 15°C, 23 to 15°C, 15 to 7°C and 15 to 23°C) (Fig. 1). Temperature treatments were achieved within a suite of adjoining climate controlled rooms, in which temperature varied ±0.5°C around the set temperature. After the 6 h temperature shift (lagged) treatment, fish in all groups were subjected to *S. parasitica* exposure as described below. Post-exposure, fish continued to be maintained at their final (prevailing)

temperature treatment until the sampling endpoint (72 h post-exposure). This experiment was performed in eight time blocks (1-4 in 2014 and 5-8 in 2015); blocks 1-4 were excluded from analyses of infection outcome due to low overt symptom rate. Fish from blocks 1-4 were processed for gene expression measurements. Analyses of gene expression were thus based on blocks carried out in 2014 and analyses of infection on blocks carried out in 2015. Final sample sizes entering analyses (excluding losses due to technical failure) are broken down by experimental cell in Table S1. All maintenance subsequent to the initial acclimation period and before challenge exposure points was in 30 L fresh water tanks at a density of <1 individual L^{-1} and subject to a 18L:6D photoperiod. Fish were fed daily (*ad libitum*) on chironomid larvae throughout the experiment.

Experiment 2 (prevailing temperature vs long-term lagged effects in the laboratory). This experiment was carried out in two blocks separate in time: in the first of these *S. parasitica* exposures were applied and in the other *G. gasterostei* exposures. Wild *G. aculeatus* were captured at RBK in February 2014 (*Saprolegnia* block) and October 2014 (*Gyrodactylus* block). Treatment and acclimatization of fish prior to experiment 2 was as for experiment 1 (see above). Acclimatized fish were weighed and measured (as above) and a random baseline sample preserved for gene expression measurements. The remaining individuals were allocated to one of 4 long-term temperature treatment (simulated winter length) groups. Over a total of 3 subsequent months, these groups were first maintained at 15°C for 0, 1, 2 or 3 months and then, respectively, at 7°C for 3, 2, 1 or 0 months (i.e., simulated winters of 0-3 months at 7°C with a synchronized end). Following this 3-month (lagged) treatment the group already at 15°C continued to be maintained at this temperature, whilst those at 7°C were raised to 15°C for the remainder of the experiment (Fig. 1). This 7-15°C transition simulated an episode of rapid early spring warming and was carried out at slightly different rates in the *Saprolegnia* and *Gyrodactylus* blocks (for operational reasons). For the *Saprolegnia* block: temperature was raised at a rate of 1-2°C day^{-1} over one week. For the *Gyrodactylus* block: temperature was raised at a rate of 0.5-1°C day^{-1} over two weeks. Groups of fish from each of the simulated winter length groups were subject to *S. parasitica* or *G. gasterostei* exposures (as described below) at the end of the long-term temperature treatment, during the warming period, and following the warming period. Average temperatures (prevailing temperature

treatments) on exposure days for the groups starting at 7°C were either 7, 7.5, 12.5 or 15°C for the *Saprolegnia* block and either 7, 9.5, 13 or 15 °C for the *Gyrodactylus* block. Final sample sizes entering analyses are broken down by experimental cell in Table S2. Post-exposure, fish continued to be subject to the wider experimental thermal regimen (acclimation to 15°C and then subsequent maintenance at 15°C) until the planned sampling endpoint. Other operational conditions were as described for experiment 1.

Experiment 3 (+2°C thermal manipulation superimposed upon natural environmental cycles in outdoors mesocosms). We utilized a system of outdoor mesocosms (12 × 300 L recirculating tanks) at Aberystwyth University, U.K. equipped with precise automatic temperature control and temperature monitoring. Six tanks were unheated, whilst another 6 were thermostatically heated to 2.0326±0.0006°C above ambient temperature (Fig. 2). Within this system we maintained separate *G. aculeatus* year cohorts (see below) in 2013-2014 (October to September) and 2014-2015 (December to November). Detailed technical specification of the recirculation, water quality management, environmental enrichment, temperature control and monitoring, stocking levels and sampling protocols are provided in Supplementary appendix S1. Briefly, fish were maintained at low biomass densities <0.05 g L^{-1}. They were fed daily with standard amounts of chironomid larvae, weekly supplemented with cladocerans. A small two-level manipulation of ration, orthogonal to the main explanatory variables of interest here, was carried out (by tank, in factorial combination with temperature treatment) as part of another study and a term for ration is included in statistical analyses below. For both iterations of the experiment post-larval young-of-the-year fish were captured in the wild at Llyn Frongoch (FRN; 52.3599,–3.8773), U.K., late in the breeding season, or after the end of the breeding season. To promote fish health during the subsequent experiment, all fish were subject to consecutive prophylactic anthelmintic praziquantel treatments (Hablützel *et al.*, 2016). Prior to the commencement of the experiment, fish were acclimatized for 4-6 weeks within the mesocosm system. Salinity was maintained throughout at 1% (10g L^{-1}) as a prophylactic measure to suppress opportunistic microbial infections. Fish were sampled monthly from the mesocosm system for gene expression measurements (October 2013 – September 2014; December 2014 – October 2015). Ten individuals per month were taken from each thermal treatment

(1-2 individuals from each tank each month, in a sequence that approximately equalized the number of fish taken from each tank in each quarter). These fish were individually netted and immediately killed by concussion and then decerebration and stored in RNA stabilization solution following Hablützel *et al.* (2016). Upon thawing (prior to gene expression analysis, see below) they were dabbed dry, weighed and measured (as above) and the abdominal cavity scanned for *Schistocephalus* plerocercoids via a ventral incision. Total weight of any plerocercoid infection was recorded and subtracted from the weight of the host. In the 2014-2015 experiment run samples of fish were removed monthly (December 2014 - October 2015), for exposure to *S. parasitica*, and separate samples of fish were removed quarterly (February, May, August, November 2015), for exposure to *G. gasterostei*. These fish were drawn in approximately equal numbers from the thermal treatments and transported to Cardiff University for experimental infection procedures. Here, fish were weighed and measured (as above) and maintained individually in 1L containers exposed to ambient thermal variation in an outdoors facility. Salt concentration of the water was reduced (from mesocosm levels) by 0.5% per day over two days, and hosts were infected after a further day in fresh water (3 days after removal from the mesocosm system). At Cardiff, all fish were fed daily, *ad libitum,* on chironomid larvae and maintained under a single temperature regimen (outside ambient); any effect of the mesocosm temperature treatment on infection outcome was thus a lagged one. Final sample sizes entering analyses are broken down by experimental cell in Table S3.

Challenge infection protocols

All experimentally challenged fish were maintained individually in standard 1 L containers with 100% water changes every 48h and fed daily (*ad libitum*) on chironomid larvae.

Saprolegnia parasitica. Isolate CBS223.65 of *S. parasitica*, derived in 1965 from *Esox lucius* was used in challenge infections. Except in experiment 2 (see next), all individual fish were subject to 30s ami-momi technique (Hatai & Hoshiai, 1993; Stueland *et al.*, 2005) to increase permissiveness to infection and then either exposed to 3×10^5 L^{-1} *S. parasitica* spore suspension for 24 h, or left non-exposed but with otherwise identical maintenance conditions (control). For experiment 2 the

following exposure conditions were used: 1) no exposure (control); 2) ami-momi treatment only; 3) exposure to *S. parasitica* spores following ami-momi treatment; 4) exposure to *S. parasitica* spores without ami-momi treatment. Spore suspensions prepared following Jiang *et al.* (2013) were generated independently for each individual fish (or less frequently for pairs of fish) directly from a central stock of CB223.65. At 72 h post-infection (p.i.) fish were individually netted and immediately killed by concussion and then decerebration. (Extensive trials indicated that fish that had not developed overt infection by 72 h p.i. did not subsequently develop symptoms.) All specimens were rapidly weighed, measured (as above) and imaged (in lateral view; digital Nikon S3600 camera) and then immediately preserved whole in RNA stabilization solution (Hablützel *et al.*, 2016) for gene expression analysis. Presence of *Schistocephalus* was determined via a ventral incision made to aid the penetration of RNA stabilization solution (see Hablützel *et al.*, 2016). Using digital images (above), the freehand selection tool in *ImageJ* (Abramoff *et al.*, 2004) was employed to measure the overall surface area of the fish and the surface area covered in erupted *S. parasitica* mycelia. Infection intensity was determined as the proportional coverage.

Gyrodactylus gasterostei. An isogenic line of *G. gasterostei*, derived from a single individual collected at RBK in October 2014 was used for experimental infections. Identification was based on morphology (Harris, 1982) and genomic sequencing (region: GenBank AJ001841.1) (Harris *et al.*, 1999). Fish were individually anaesthetized in 0.02% MS222. Then, using a dissecting microscope and fibre-optic lighting, the caudal fins of an infected donor and recipient fish were overlaid until 2 individuals of *G. gasterostei* transferred to the caudal fin of the recipient. Infected fish were screened 24 h p.i. in fresh water under anaesthesia (0.02% MS222) and body surfaces checked for infection; fish uninfected after this initial examination were re-infected. Subsequently, fish were screened every 5 days for 91 days in experiment 2 and every 4-5 days for 58 days in experiment 3. At the experimental endpoints fish were killed, weighed and measured (as above), and dissected to record parasites in the body cavity, swim bladder, gut, gills and eyes (the only co-infecting parasite recovered was *S. solidus*). *G. gasterostei* is predominantly a parasite of external body surfaces (>7000 fish examined from RBK have never contained this common species in the branchial cavity; JC per. obs.).

Thermal acclimation of parasites. Source *Saprolegnia* and *Gyrodactylus* cultures were maintained at a single intermediate temperature (15°C) prior to experiments to provide infectious challenges with a standardized thermal reaction norm (given the possibility of acclimation effects (Altman *et al.*, 2016)).

Naturally-acquired infections persisting in experimental fish

Schistocephalus solidus plerocercoid larva infections were refractory to the prophylactic treatments described above and were the only naturally-acquired macroparasite to carry over significantly into the experiments (*S.solidus* would have been unable to transmit within experiments due to its indirect life cycle). Presence of other macroparasites and overt microbial infections was confirmed to be at negligible levels (<5% prevalence) through visual monitoring of experimental fish, direct parasitological examination at endpoints (where sampling procedures allowed), and by examination of animals prepared for, but unused in, experiments. The presence of *S. solidus* infection was recorded in all experiments (see above) and included in statistical analyses.

Ethics

Work involving animals conformed to U.K. Home Office (HO) regulations; elements at Aberystwyth University were approved by the animal welfare committee of the Institute of Biological, Environmental and Rural Sciences (IBERS), Aberystwyth University and conducted in consultation with the HO inspectorate; elements at Cardiff University were approved by the Cardiff University Ethics Committee and conducted under HO licence PPL 302357.

Gene expression measurements

We measured expression of 14 immune-associated genes using quantitative real-time PCR as previously described (Hablützel *et al.*, 2016). The immunological roles of the genes are summarized in Table S4.

Analyses

All analyses were carried out in *R* version 3.2.3. In the statistical analysis of our experimental results we employed linear mixed models (LMMs, package *lme4*) or general linear models (LMs) for the confounder-adjusted analysis of gene expression

responses (the latter if no random term was significant). Power transformations derived via a Box-Cox procedure were applied to individual expression variables on a case-by-case basis following evaluation of standard model diagnostics. In a few cases skewed gene expression variables containing some zeros were analysed in generalized additive models for location, scale and shape (Rigby & Stasinopoulos, 2005, Stasinopoulos & Rigby, 2007) (GAMLSS) with a zero-adjusted gamma distribution (using the package *gamlss*). For *Saprolegnia* infections we considered the proportion of body surface coverage by erupted mycelia and analysed these data in GAMLSS models. The latter employed a zero-inflated beta distribution incorporating parameters for the probability (α) of not developing overt symptoms (erupted mycelia) and also for the severity of symptoms (location parameter, μ, reflecting coverage by mycelia in overt cases). For *Gyrodactylus* we considered demographic parameters for continuously monitored individual infrapopulations (time to peak infection and peak infection abundance) analysing these data in LMs with a ($\log_{10} + 1$) transformation. *Schistocephalus* infection data (total infection weight per host, parasitic index [total infection weight / host weight]) were analysed in LMs, or in generalized additive models (GAM) (Wood, 2006) when irregular trends were better represented by non-parametric smoothers (package *mgcv*) (random intercept terms for tank were not significant in these analyses). Except where otherwise stated, statistical analyses of gene expression and infection metrics included explanatory terms for the following in starting models: host length, sex, body condition (calculated as residuals from a quadratic regression of weight on length), *Schistocephalus* infection if this was present in the sample (present/absent; and except where this infection was the analysed response), reproductive condition (breeding / non-breeding condition; only in the long-term experiment 3), factorial experimental treatments and experimental block (experiment 1) or year (experiment 3); sampling (tank) and assaying (assay plate) structure was represented with random intercept terms, where relevant. Interaction terms of interest were included where specified below. The model for *Saprolegnia* infection in experiment 2 was developed using just the thermal treatment terms and host terms significant in experiment 1, due to limited sample size. Models for gene expression in experiments 1 and 2 included factors representing exposure to, and overt infection with, *Saprolegnia*; the experiment 2 analysis contained a fixed term for time (in degree days) within the experiment. Random terms were assessed (in the full model) by likelihood ratio tests in LMMs

and GAMLSSs. When a random effect was added to a GAM as penalized regression terms (to give a generalized additive mixed model, GAMM), its importance was assessed by Akaike information criterion (AIC). Fixed model terms were retained based on AIC for LMs, GAMLSSs and GAMs and *F*-tests (with Satterthwaite's approximation to degrees of freedom) for LMMs. Reported *P* values were determined by likelihood ratio tests in GAMLSSs, *F* tests in LMs, *F* tests with Satterthwaite's approximation in LMMs and Wald tests in GAMs. Standard diagnostic plots of residual and fitted values and quantile-quantile plots of residuals were inspected for all models.

A sinusoid model (1) was employed to explicitly represent the possibility that the direct thermal effect on resistance to *Saprolegnia* (α; probability of resisting overt infection following exposure), as observed in laboratory experiments 1 and 2, was counteracted by other seasonal environmental influences on host immunocompetence in experiment 3:

Saprolegnia α = *x* + Immunocompetence driver (ID) + Thermal driver (TD) (1)

$$\mathrm{ID} = c \times a \times \cos\left[\left(\frac{2\pi t}{12}\right) - \theta^{1}\right]$$

$$\mathrm{TD} = d \times E$$

$$E = b \times \cos\left[\left(\frac{2\pi t}{12}\right) - \theta^{2}\right]$$

Where E is environmental temperature (°C), *Saprolegnia* α is the monthly probability of resisting overt *Saprolegnia* symptoms and *t* is time (months) (all observed in experiment 3); parameters are detailed in Table 1. Given the seasonal nature of temperature and *Saprolegnia α* variation in experiment 3, this model represents a temperature driver (TD) and a putative immunocompetence driver (ID) with separate (superimposed) annual sinusoid functions (Stolwijk *et al.*, 1999). We parameterized the amplitude and acrophase of TD from our records of temperature (using parameter estimates from cosinor regression of temperature against time, see below) and the thermal coefficient, *d* (converting temperature into α, see Table 1), from laboratory experiments (using an intermediate value based on analysis of experiments 1 and 2). Taking an inverse modelling approach we then fitted this

partially parameterized model (1) to the monthly *Saprolegnia* α data (from experiment 3) and estimated parameters associated with ID. For this we used package *FME* (Soetaert & Petzoldt, 2010) to carry out constrained fitting of the model. Cosinor regression (Tong, 1976) was carried out with package *cosinor* in order to estimate the amplitude and acrophase of seasonal temperature variation.

As descriptors of thermal variability in the 7-day windows preceding sampling points in experiment 3 we considered temperature variance, amplitude of diel temperature variation, the shape of the time series represented by Fourier coefficients, and the maximum upward trend (given that in experiment 1 we observed a protective effect of upward temperature shifts).To quantify diel temperature variation we fitted a GAM to each time series, with parametric sinusoidal time terms to represent diel oscillation and a non-parametric smoother for time to represent other temporal trends (Wood, 2006). Amplitude of the diel oscillation was calculated from the parameters of the sinusoidal terms (Stolwijk *et al.*, 1999). Between-month distances based on Fourier coefficients (FCD) were calculated from centred time series using package *TSdist* (Mori *et al.*, 2017).

Results

The prevailing temperature consistently had substantial effects on infection and immunity under controlled laboratory conditions

Both experiments 1 and 2 included factorial combinations of prevailing and lagged thermal treatments. Considering the main effects of prevailing temperature first, we found that most immune-associated genes (12/14) (Fig. 3a, Table 2; Fig. S2) showed significant change in expression across the range 7-23°C (experiment 1) and many (6/14) (Fig. 3a, Table 3; Fig. S3) did across the range 7-15°C (experiment 2). These expression changes were consistent with monotonic responses (Fig. S2-S3). The broad effect size of prevailing temperature on gene expression was substantial: temperature variation across the range 7-23°C had a similar impact to sex and greater impact than other host variables such as size, body condition and infection status (Fig. S4).

In *Saprolegnia* challenges (Fig. 3b-c), resistance to overt disease (α parameter) became less probable with increasing prevailing temperature in both laboratory experiments (GAMLSS analyses; experiment 1, α = -0.12±0.04, $P = 2.9 \times 10^{-3}$, experiment 2, α = -1.05±0.46, $P = 1.1 \times 10^{-5}$). In *Gyrodactylus* challenges in experiment 2, low temperature exposure during the early stages of established infection produced a more severe outcome: parasite abundance peaking later and higher (Fig. 3f, g) (LMs; $\log_{10}$ time to peak = -0.04±0.01, $P = 6.1 \times 10^{-3}$; $\log_{10}$ peak population = -0.07±0.02, $P = 9.5 \times 10^{-4}$). Notably, data presented by Harris (1982) indicate that *G. gasterostei* infrapopulations also peak later and higher when maintained at a constant temperature of 10 compared to 15°C. The direction of these thermal effects on peak parasite numbers is contrary to the expectation that such a temperature increase would promote *Gyrodactylus* population growth in permissive conditions (Harris, 1982; Gelnar, 1990; Jackson & Tinsley, 1994; Sereno-Uribe *et al.*, 2012), and indicative that low temperature impairs the early development of resistance responses (Andersen & Buchmann, 1998).

Lagged effects of past temperature on infection and immunity were detectable but not consistently important

Some main effects of lagged thermal treatments were evident in the gene expression results in both laboratory experiments (Fig. 3a, Tables 2-3). However, lagged thermal effects occurred much less frequently (Fig. 3a) than prevailing temperature effects (14 genes showed significant prevailing effects and 6 genes significant lagged effects in one or both of experiment 1 and 2). There were no effects on gene expression due to interactions between prevailing temperature and preceding temperature treatments in either experiment.

There were no lagged main effects of temperature on *Saprolegnia* infections in experiments 1 or 2. This was with the exception of a single scenario: where rapid upward shifts in temperature in experiment 1 had a protective effect (increasing α) (Fig. 3d) (GAMLSS analysis; +8°C shift α = 3.92±1.20, reference level = -8°C shift; term deletion $P = 1.1 \times 10^{-4}$). For *Gyrodactylus* in experiment 2 we found no effect of past temperatures previous to the period of infection (i.e., of simulated winter length) on infrapopulation dynamics. No interactions occurred between lagged temperature

and prevailing temperature treatments for *Saprolenia* (experiments 1-2) or *Gyrodactylus* (experiment 2).

Thermal effects on infection and immunity were readily detectable in a realistic warming scenario superimposed upon natural environmental cycles

Turning to our mesocosm experiment we first asked what effect the +2°C manipulation (simulating climate warming) had on gene expression and infection outcomes. We found that several genes responded significantly (*cd8a*, *il12ba*, *defbl2*, *tbk1*; always in the same direction as responses in laboratory experiments), even against the background of natural seasonal variation (Fig. 3a; Table 4). For *Schistocephalus* infections *in situ* within the mesocosms, the direct effect of the +2°C increment increased the parasitic index (infection weight/host weight, PI) (Fig. 3h) (LM; +2°C 0.095±0.023, $P = 1.1 \times 10^{-4}$) and pleroceroid weight (GAM; +2°C 10.9±4.6, $P = 0.02$) although without the extreme plerocercoid size increases reported in recent constant temperature experiments (Macnab & Barber, 2012). There was no lagged main effect of the +2°C temperature manipulation on *Saprolegnia* and *Gyrodactylus* infection outcomes in fish extracted from the mesocosms and equalized to the same (natural) temperature regimen before exposure to infection. However, there was a significant month × lagged temperature treatment interaction for symptom severity in *Saprolegnia* (μ parameter), with modulated infection outcomes in the winter and late summer (Fig. 3e) (GAMLSS; +2°C × month: Feb^{low} -1.69±0.81, Aug^{low} 2.400±1.16, Sept^{low} -3.90±1.15; term deletion $P = 7.9 \times 10^{-4}$).

Given thermal responses observed in the laboratory, disease progression was paradoxically highest in winter in an environment with natural seasonality

We next asked how well the year-round patterns of infection susceptibility seen in mesocosms (experiment 3) corresponded to the observed responses in our laboratory manipulations of temperature. In the more realistic mesocosm setting there was striking evidence that seasonal trends were superimposed upon direct thermal effects, leading to results unpredictable on the basis of thermal variation alone (Zimmerman *et al.*, 2010). Thus, the probability of resisting overt *Saprolegnia* infection (α parameter), which decreased when temperature was increased in the laboratory (Fig. 3b, c), paradoxically was lowest during winter in the mesocosms

(Fig. 4a) (GAMLSS; α Feb - 2.49±0.79; month term deletion, $P = 1.8 \times 10^{-4}$). A corresponding pattern was seen in *in situ Schistocephalus* infections in the mesocosms. As described above (see also Fig. 3h), the +2°C temperature manipulation produced an increase in PI, indicating a positive thermal dependence of disease severity (as for *Saprolegnia* α). Contrary to this thermophilic trend, though, PI in fact increased during the winter months (Fig. 3h) and ceased to increase thereafter (LM with quadratic term for time; time 0.056±0.015, $P = 0.014$; time^2 -0.004±0.001, $P = 2.7 \times 10^{-3}$). This pattern is consistent with lowered host resistance during winter and rapid plerocercoid growth (relative to the host) despite low winter temperatures. For both *Saprolegnia* and *Schistocephalus*, the pattern of results is thus suggestive of a seasonal immunocompetence variable (low host immunocompetence in winter) that acts in opposition to the direct effects of prevailing environmental temperature (positive thermal dependence of host exploitation, as demonstrated in experiments 1 and 2). For *Gyrodactylus,* as for *Saprolegnia* and *Schistocephalus*, the worst disease also occurred in winter (Fig. 4b, c), with infection abundance peaking later (LM; $\log_{10}$ time to peak, Aug 0.14±0.09, Nov 0.21±0.08, Feb 0.30±0.077, reference May; month term deletion $P = 9 \times 10^{-4}$) and higher (LM; $\log_{10}$ peak population; Aug 0.17±0.15, Nov 0.32±0.14, Feb 0.43±0.12; $P = 0.007$).

A latent seasonal immunocompetence variable, that correlated with immune gene expression and opposed thermal effects, explained winter-biased disease progression in natural circumstances

We set out to explicitly partition seasonal thermal and immunocompetence effects contributing to the winter-biased pattern of infection susceptibility seen in experiment 3. We focussed on *Saprolegnia*, for which most experimental data were available and for which the binary infection endpoint (α) simplified interpretation. As seasonal fluctuation can be represented with sinusoid functions (Stolwijk *et al.*, 1999), we constructed a model explaining the (logit scale) *Saprolegnia* α parameter in terms of a cosine wave for annual thermal variation and another cosine wave for seasonally-varying immunocompetence (see (1), Table 1, Fig. 5). We first parameterized the amplitude and acrophase of the annual temperature function from our 2014-2015 temperature monitoring data and estimated the coefficient converting this into infection rate from observations on the effect of prevailing temperature in

experiments 1 and 2. (We did not include lagged thermal effects because of the lack of these in experiments 1 and 2, except for the protective effect of previous sharp warming; although we do examine the latter, and other aspects of thermal variance, further below.) We then used an inverse modelling approach to compute the parameters of the latent immunocompetence function by fitting the partially parameterized model to our 2014-2015 *Saprolegnia* infection data. The fully parameterized model explained 22% of the variation in *Saprolegnia* α, and suggested that effects driven by temperature and by seasonal immunocompetence were almost collinear (Fig. 5). Importantly, we note that the distinct contributions of temperature and immunocompetence would therefore have been unobservable had only infection data been available (as in many field studies).

We considered whether the latent immunocompetence variable derived above might represent the protective lagged effect of sharp temperature rises, as observed in experiment 1, or of other aspects of preceding temperature variability, but found this to be unlikely. As immunocompetence and prevailing temperature were collinear (see above), we expected that any component of temperature variability predominantly driving immunocompetence would necessarily be correlated with prevailing temperature. Therefore, we examined different descriptors of temperature variability (in the week before monthly sample points) for this correlation.

The maximum upward trend, variance and shape (FCD) of monthly temperature time series (in the week before sampling) were not associated with mean monthly prevailing temperature (Fig. 6a-c). Although the amplitude of diel temperature variation did increase with temperature (Fig. 6d), the absolute size of this increase was small (~ 1°C across the annual thermal range; corresponding to a ~ 2°C diel range difference) when considered in the light of the effect size for a +8°C shift on *Saprolegnia* α in experiment 1. The latter corresponded to a change in α of 0.8 across 2°C (the annual diel range difference), compared to an annual α range of >5 for the immunocompetence driver shown in Fig. 5a.

We also asked whether the latent immunocompetence variable was associated with independent data for the expression of immunity genes. We found that one gene, *ighm* (P = 0.003) (Fig. 5b), was clearly associated and that four others were more marginally associated: *il4* (P = 0.07), *tirap* (P = 0.04), *defbl2* (P = 0.06) and *cd8a* (P

= 0.06) (in confounder-adjusted LMMs, with random intercepts for month). In all of these cases, increased expression corresponded to increased latent immunocompetence. The association with *ighm* is consistent with the suspected involvement of antibodies in resistance to *Saprolegnia* infection (Minor *et al.*, 2014) and with elevated early autumn anti-*Saprolegnia* antibody seropositivity in wild salmonids (Fregeneda-Grandes *et al.*, 2009).

Discussion

We focussed on the three-spined stickleback and its pathogens as a natural experimental model. We readily detected perturbation of immune expression and infectious disease progression in a realistic experimental climate warming scenario applied in naturalistic outdoors mesocosms. Even for a modest thermal increment (+2°C), significant expression differences were observed for 4/14 immune-associated genes examined (*cd8a*, *tbk1*, *il12ba*, *defbl2*) whilst *Schistocephalus* parasitic index and plerocercoid growth increased. Lagged thermal effects on *Saprolegnia* symptom severity (μ) also featured in a significant interaction with month. This interaction reflected a distinctive seasonal pattern of disease progression in the warmed environment, demonstrating the potential for change in the phenology of disease (Buehler *et al.*, 2008; Paull & Johnson, 2014) under climate warming.

In CBVs like the three-spined stickleback, within-host infection dynamics can thus be expected to respond appreciably to rapid year-on-year warming. Direct thermal effects may drive part of this response, which in turn contributes to population- (Barber *et al.*, 2016; Mignatti *et al.*, 2016) and community-level (Karvonen *et al.*, 2013; Paull & Johnson, 2014) pathogen dynamics. But these higher-level responses will also depend on other factors: on thermal responses of free-living transmission stages and on indirect effects of temperature (on both within-host and free-living stages) mediated through changes in the environment. It is important (as we describe below in the case of thermal and non-thermal environmental influences on *Saprolegnia* disease progression) to decompose such complex composite processes into their fundamental parts, if we are to understand the sources of dynamical change in natural systems.

To estimate thermal effects (holding other environmental effects constant) we carried out laboratory experiments with factorial combinations of lagged and prevailing temperature treatments. The controlled conditions in these experiments would have prevented the formation of seasonal environmental variation (e.g., plankton development) as occurred in the mesocosm experiment. The laboratory experiments, together with the mesocosm experiment (above), not unexpectedly (Bly & Clem, 1992; Maniero & Carey, 1997; Le Morvan *et al.*, 1998; Makrinos & Bowden, 2016) confirmed a major general effect of temperature in modulating immunity and within-host infectious disease outcomes in CBVs. All of the 14 gene expression measures and all 3 infection systems that we examined showed some significant response to experimental manipulation of temperature, in many cases with substantial effect sizes. Whilst other studies of ectothermic organisms have emphasized the importance of lagged thermal influences on immunity, we found that thermal effects were mediated most powerfully by the prevailing temperature. Overall, less than half the number of genes (in experiments 1 and 2) showed expression responses to past thermal variation as to prevailing temperature. All three of our infection systems showed the effect of temperature prevailing within the timeframe of infection, but there were few cases in which temperature prior to this timeframe was important. Amongst the lagged thermal treatments in our laboratory experiments only sharp temperature rises had any significant effect: decreasing the probability of developing of overt *Saprolegnia* infection. As discussed above, there was also an interaction between lagged thermal treatment and *Saprolenia* symptom severity (μ) in the mesocosm experiment. Putting these results in perspective, we note that the lagged temperature treatments we used in laboratory experiments (simulated winters 0-3 months long and 8°C thermal shifts over 6 h) were relatively extreme. This would have exaggerated the importance of lagged compared to prevailing temperature effects, as the latter were represented in our experiments by a set of values well within the natural range. Interestingly we did not find an anti-protective effect of sharp temperature falls on *Saprolegnia* infection. Whilst such a tendency has been reported in saprolegniosis of channel catfish (Bly *et al.*, 1992), and in fungal infections of lower vertebrates (Raffel *et al.*, 2013), our results suggest this effect is not a general one. Even leaving the effects of the non-thermal variation (see below) aside, our data indicate that past temperature records will be of limited use for managers of CBV populations in projecting infectious disease susceptibility.

Rather systems for the projection of disease risk based on prevailing temperature variation will be more effective.

Combining our mesocosm and laboratory experimental data we considered the contributions of thermal and non-thermal environmental variation to disease progression. Importantly, in the outdoors mesocosm environment (subject to biotic and abiotic seasonality), *Saprolegnia* and *Schistocephalus* infections occurred in a pattern not explained by their responses to experimental thermal manipulations. In both infections disease progression was increased by upwards experimental manipulation of temperature, all other things being equal, but under mesocosm conditions was also at its greatest in winter. Crucially, our study design allowed us to partition thermal effects from other environmental effects on disease progression, revealing their relative magnitude. Using an inverse modelling approach to represent monthly *Saprolegnia* challenge infection outcomes in the outdoor mesocosms, and including (prevailing) thermal effects parameterized from our laboratory experiments, we were able to derive a seasonal latent variable opposing (and slightly outbalancing) thermal effects. This variable represented environmental effects on anti-*Saprolegnia* immunocompetence, other than those due to the prevailing temperature, and reconciled laboratory and mesocosm observations. It could not be explained by seasonal patterns of temperature variance (cross-referencing to effects observed in laboratory experiments), and was independently (positively) correlated with monthly expression of the immunoglobulin M heavy chain gene *ighm*. This is of note because of the likely relevance of IgM for resistance to *Saprolegnia* (Minor *et al.*, 2014). Furthermore, as teleost IgM antibodies may have a short half-life (1-3 days) (Voss Jr *et al.*, 1980; Ye *et al.*, 2010, 2013), a link between levels of heavy chain mRNA and functional antibody is not unrealistic.

Thus, the non-thermal environmental contribution (via seasonal immunocompetence effects) to *Saprolegnia* disease progression variance is large (of similar size to the thermal contribution, slightly outbalancing it across the year). Whilst it is beyond the scope of the present study to determine the environmental agents involved, such seasonal variation in immunity is well known in other vertebrate systems (Beldomenico *et al.*, 2008; Martin *et al.*, 2008). It should be pointed out, moreover, that although some seasonal variation in the expression of immunity genes occurs in

mesocosm fish, we have previously observed such responses to be diminished compared to those in the wild (Hablützel *et al.*, 2016). This suggests that the component of disease progression variation determined by non-thermal environmental effects on immunocompetence, and not directly by temperature, may be even larger under fully natural conditions in the wild.

We note, additionally, the variable sign in the disease responses of our 3 infection systems to prevailing temperature manipulations (positive for *Saprolegnia* α and *Schistocephalus* parasitic index and negative for *Gyrodactylus* abundance). This is consistent with the simple theoretical scenario, introduced at the beginning, where disease worsens or ameliorates determined by the interplay of species-specific thermal reaction norms in host and pathogen (Jackson & Tinsley, 2002). Whilst some previous studies have emphasized the magnifying effects of warming temperature regimens on host susceptibility in specific systems (Macnab & Barber, 2012), it is also possible to find examples where rising temperature increases resistance (Jackson & Tinsley, 2002; Douglas *et al.*, 2003; Raffel *et al.*, 2013). Furthermore, in other cases infectious disease may show convex responses to temperature, for example with symptoms emerging across a limited temperature range (Gilad *et al.*, 2003; Ito & Maeno, 2014). This can result from non-linear thermal reaction norms in host and or parasite. Thus, although thermal change, all other things being equal, readily shifts the burden of disease caused by individual pathogen species, the direction of these shifts may not be consistent, and the overall disease outcome in host-parasite communities is likely to play out in a system specific way.

Elements of our results also provide an additional perspective to those of (Dittmar *et al.*, 2014) who examined head kidney (HK) cell responses and immune gene expression in *G. aculeatus* under different thermal regimens and with an emphasis on the upper end of the natural temperature range. These authors concluded that high levels of certain HK cellular responses at 13°C corresponded to high immunocompetence and that increased gene expression responses at higher temperatures (correlating negatively with body condition) were indicative of immunopathology and dysregulation. This interpretation for cellular responses is partly consistent with our laboratory results. For example, under our present study

conditions, both *Saprolegnia* and *Schistocephalus* disease progression worsened as the temperature rose (all other things being equal), although this could also relate to the cold-biased expression of some innate immune pathways that we observed here. On the other hand, we found that under natural circumstances (in mesocosms) high expression of adaptive immunity genes (such as *ighm*) correlated with high immunocompetence and also coincided with the warmest times of year. Furthermore, in late summer (in the weeks following seasonal peaks in temperature) we have not found fish exposed to natural temperature variation to undergo marked reductions in condition (Hablützel *et al.*, 2016). Rather the genome-wide transcriptomic signatures seen in wild fish at this time of year include adaptive immune activity and also growth and development (Brown *et al.*, 2016), the latter indicative of robust health. Taken together, these observations suggest that, within the normal range of temperatures (although perhaps not at the more extreme temperatures considered by Dittmar *et al.*), high immune gene expression does not necessarily equate to dysregulation and may reflect effective resistance responses.

In conclusion, we generated a realistic mid-latitude climatic warming scenario in outdoors mesocosms, incorporating precise temperature control. With this we demonstrated significant perturbation of immunity and infectious disease progression under modest incremental warming (+2°C) in a representative natural model CBV (the three-spined stickleback). These perturbations included changes in both the magnitude and phenology of disease that might be of practical importance in real-world situations. Parallel laboratory experimental analyses confirmed that thermally-driven responses of immunity and infectious disease progression were substantial. When all else was equal, thermal effects were most strongly dependent on the prevailing temperature (the latter, in the case of infection, here taken to encompass temperature regimen post-invasion). Lagged thermal effects (preceding invasion, in the case of infection) were less important. The contrasting responses to thermal manipulation of our different infection systems confirm that increases in temperature can worsen or ameliorate disease progression according to the specific thermal biology of the host and pathogen. Thus, in an otherwise constant warming environment, within-host outcomes would likely to play out in a system-specific way in complex host-parasite communities, without necessarily increasing the overall burden of disease. Most importantly, by combining our mesocosm observations with

experimentally-derived estimates of thermal effects, we show that, in a seasonal natural system, thermal effects are superimposed upon substantial temporal variation in immunocompetence. The latter is driven by non-thermal aspects of the environment and, for *Saprolegnia*-mediated disease, its effect is at least as large as that of thermal variation. Critically, thermal change is likely to indirectly affect the non-thermal environmental drivers of immunocompetence, additional to its direct effects on disease progression. Thus, projection of infection dynamics based on experimentally-determined thermal effects alone is unlikely to be reliable, given the size of non-thermal environmental effects on immunocompetence. In practical management situations, the accuracy of such projections might be improved by primarily considering prevailing (and not lagged) thermal effects and by incorporating validated measures of immunocompetence (such as *ighm* expression in the case of *Saprolegnia* here).

Acknowledgements

Work was funded by research grants from the Leverhulme Trust (RPG-301) and the Fisheries Society of the British Isles. We thank Rory Geohagen, Rob Darby and Gareth Owen (Aberystwyth University) and Robby Mitchell (Cardiff University) for assistance. We also thank Chris Williams (Environment Agency, UK) for advice, Pieter van West for providing a *Saprolegnia parasitica* culture and Mike Begon for comments.

References

Abramoff MD, Magalhães PJ, Ram SJ (2004) Image processing with ImageJ. *Biophotonics international,* **11**, 36-42.

Altman KA, Paull SH, Johnson PTJ, Golembieski MN, Stephens JP, Lafonte BE, Raffel TR (2016) Host and parasite thermal acclimation responses depend on the stage of infection. *Journal of Animal Ecology,* **85**, 1014-1024.

Andersen PS, Buchmann K (1998) Temperature dependent population growth of *Gyrodactylus derjavini* on rainbow trout, *Oncorhynchus mykiss*. *Journal of Helminthology*, **72**, 9-14.

Barber I, Berkhout BW, Ismail Z (2016) Thermal change and the dynamics of multi-host parasite life cycles in aquatic ecosystems. *Integrative and Comparative Biology,* **56**, 561-572.

Barber I, Scharsack JP (2010) The three-spined stickleback-*Schistocephalus solidus* system: an experimental model for investigating host-parasite interactions in fish. *Parasitology,* **137**, 411-424.

Beldomenico PM, Telfer S, Gebert S, Lukomski L, Bennett M, Begon M (2008) The dynamics of health in wild field vole populations: a haematological perspective. *Journal of Animal Ecology*, **77**, 984-997.

Bly JE, Clem LW (1992) Temperature and teleost immune functions. *Fish and Shellfish Immunology,* **2**, 159-171.

Bly JE, Lawson LA, Dale DJ, Szalai AJ, Durburow RM, Clem LW (1992) Winter saprolegniosis in channel catfish. *Diseases of Aquatic Organisms,* **13**, 155-164.

Brown M, Hablützel P, Friberg IM, Thomason AG, Stewart A, Pachebat JA, Jackson JA (2016) Seasonal immunoregulation in a naturally-occurring vertebrate. *BMC Genomics,* **17**, 1-18.

Buehler DM, Piersma T, Matson K, Tieleman BI (2008) Seasonal redistribution of immune function in a migrant shorebird: annual-cycle effects override adjustments to thermal regime. *American Naturalist,* **172**, 783-796.

Dittmar J, Janssen H, Kuske A, Kurtz J, Scharsack JP (2014) Heat and immunity: an experimental heat wave alters immune functions in three-spined sticklebacks (*Gasterosteus aculeatus*). *Journal of Animal Ecology,* **83**, 744-757.

Douglas CW, Ross AA, Gerry M (2003) Emerging disease of amphibians cured by elevated body temperature. *Diseases of Aquatic Organisms,* **55**, 65-67.

Fregeneda-Grandes JM, Carbajal-Gonzalez MT, Aller-Gancedo JM (2009) Prevalence of serum antibodies against *Saprolegnia parasitica* in wild and farmed brown trout *Salmo trutta*. *Diseases of Aquatic Organisms,* **83**, 17-22.

Garner TWJ, Rowcliffe JM, Fisher MC (2011) Climate change, chytridiomycosis or condition: an experimental test of amphibian survival. *Global Change Biology,* **17**, 667-675.

Gelnar M (1990) Experimental verification of the water temperature effect on the micropopulation growth of *Gyrodactylus rutilensis* Glaser, 1974 (Monogenea). *Folia Parasitologica (Praha),* **37**, 113-114.

Gilad O, Yun S, Adkison MA, Way K, Willits NH, Bercovier H, Hedrick RP (2003) Molecular comparison of isolates of an emerging fish pathogen, koi herpesvirus, and the effect of water temperature on mortality of experimentally

infected koi. *Journal of General Virology,* **84**, 2661-2667.

Hablützel IP, Brown M, Friberg IM, Jackson JA (2016) Changing expression of vertebrate immunity genes in an anthropogenic environment: a controlled experiment. *BMC Evolutionary Biology,* **16**, 1-12.

Harris P (1982) Studies of the Gyrodactyloidea (Monogenea). Unpublished Ph. D. University of London.

Harris PD, Cable J, Tinsley RC, Lazarus CM (1999) Combined ribosomal DNA and morphological analysis of individual gyrodactylid monogeneans. *Journal of Parasitology,* **85**, 188-191.

Hatai K, Hoshiai G-I (1993) Characteristics of two *Saprolegnia* species isolated from Coho salmon with saprolegniosis. *Journal of Aquatic Animal Health,* **5**, 115-118.

IPCC (2014) Climate Change 2014: Synthesis Report. Contribution of Working Groups I, II and III to the Fifth Assessment Report of the Intergovernmental Panel on Climate Change. Geneva, Switzerland, IPCC.

Ito T, Maeno Y (2014) Effects of experimentally induced infections of goldfish *Carassius auratus* with cyprinid herpesvirus 2 (CyHV-2) at various water temperatures. *Diseases of Aquatic Organisms,* **110**, 193-200.

Jackson JA, Tinsley RC (1994) Infrapopulation dynamics of *Gyrdicotylus gallieni* (Monogenea: Gyrodactylidae). *Parasitology,* **108**, 447-452.

Jackson JA, Tinsley RC (2002) Effects of environmental temperature on the susceptibility of *Xenopus laevis* and *X. wittei* (Anura) to *Protopolystoma xenopodis* (Monogenea). *Parasitology Research,* **88**, 632-638.

Jiang RH, De Bruijn I, Haas BJ *et al.* (2013) Distinctive expansion of potential virulence genes in the genome of the oomycete fish pathogen *Saprolegnia parasitica*. *PLoS Genetics,* **9**, e1003272.

Karvonen A, Kristjánsson BK, Skúlason S, Lanki M, Rellstab C, Jokela J (2013) Water temperature, not fish morph, determines parasite infections of sympatric Icelandic threespine sticklebacks (*Gasterosteus aculeatus*). *Ecology and Evolution,* **3**, 1507-1517.

Le Morvan C, Troutaud D, Deschaux P (1998) Differential effects of temperature on specific and nonspecific immune defences in fish. *Journal of Experimental Biology,* **201**, 165-168.

Macnab V, Barber I (2012) Some (worms) like it hot: fish parasites grow faster in

warmer water, and alter host thermal preferences. *Global Change Biology,* **18**, 1540-1548.

Makrinos DL, Bowden TJ (2016) Natural environmental impacts on teleost immune function. *Fish and Shellfish Immunology,* **53**, 50-57.

Maniero GD, Carey C (1997) Changes in selected aspects of immune function in the leopard frog, *Rana pipiens*, associated with exposure to cold. *Journal of Comparative Physiology B,* **167**, 256-263.

Martin LB, Weil ZM, Nelson RJ (2008) Seasonal changes in vertebrate immune activity: mediation by physiological trade-offs. *Philosophical transactions of the Royal Society of London. Series B, Biological Sciences,* **363**, 321-339.

Mignatti A, Boag B, Cattadori IM (2016) Host immunity shapes the impact of climate changes on the dynamics of parasite infections. *Proceedings of the National Academy of Sciences of the United States of America,* **113**, 2970-2975.

Minor KL, Anderson VL, Davis KS *et al.* (2014) A putative serine protease, SpSsp1, from *Saprolegnia parasitica* is recognised by sera of rainbow trout, *Oncorhynchus mykiss*. *Fungal Biology,* **118**, 630-639.

Mori U, Mendiburu A, Lozano JA (2017) Distance measures for time series in R: the TSdist package. *The R Journal*, **8/2**, 451-459.

Murdock CC, Paaijmans KP, Bell AS, King JG, Hillyer JF, Read AF, Thomas MB (2012) Complex effects of temperature on mosquito immune function. *Proceedings of the Royal Society of London. Series B, Biological sciences*, **279**, 3357-3366.

O'Reilly CM, Sharma S, Gray DK *et al.* (2015) Rapid and highly variable warming of lake surface waters around the globe. *Geophysical Research Letters,* **42**, 10,773-710,781.

Paull SH, Johnson PTJ (2014) Experimental warming drives a seasonal shift in the timing of host-parasite dynamics with consequences for disease risk. *Ecology Letters,* **17**, 445-453.

Podrabsky JE, Somero GN (2004) Changes in gene expression associated with acclimation to constant temperatures and fluctuating daily temperatures in an annual killifish *Austrofundulus limnaeus*. *Journal of Experimental Biology,* **207**, 2237-2254.

Raffel TR, Halstead NT, Mcmahon TA, Davis AK, Rohr JR (2015) Temperature variability and moisture synergistically interact to exacerbate an epizootic

disease. *Proceedings of the Royal Society of London. Series B, Biological Sciences,* **282**, 20142039.

Raffel TR, Rohr JR, Kiesecker JM, Hudson PJ (2006) Negative effects of changing temperature on amphibian immunity under field conditions. *Functional Ecology,* **20**, 819-828.

Raffel TR, Romansic JM, Halstead NT, Mcmahon TA, Venesky MD, Rohr JR (2013) Disease and thermal acclimation in a more variable and unpredictable climate. *Nature Climate Change,* **3**, 146-151.

Rigby RA, Stasinopoulos DM (2005) Generalized additive models for location, scale and shape. *Journal of the Royal Statistical Society: Series C (Applied Statistics),* **54**, 507-554.

Roberts RJ (2012) *Fish Pathology,* Chichester, John Wiley & Sons.

Robertson S, Bradley JE, Maccoll AD (2016) Measuring the immune system of the three-spined stickleback - investigating natural variation by quantifying immune expression in the laboratory and the wild. *Molecular Ecology Resources,* **16**, 701-713.

Scheiner SM (1993) Genetics and evolution of phenotypic plasticity. *Annual Review of Ecology and Systematics*, **24**, 35-68.

Sereno-Uribe AL, Zambrano L, Garcia-Varela M (2012) Reproduction and survival under different water temperatures of *Gyrodactylus mexicanus* (Platyhelminthes: Monogenea), a parasite of *Girardinichthys multiradiatus* in Central Mexico. *Journal of Parasitology,* **98**, 1105-1108.

Sharma S, Gray DK, Read JS *et al.* (2015) A global database of lake surface temperatures collected by in situ and satellite methods from 1985-2009. *Scientific Data,* **2**, 150008.

Shinn AP, Bron JE (2012) Considerations for the use of anti-parasitic drugs in aquaculture. In: *Infectious disease in aquaculture* (ed. Austin B), pp. 190-217. Woodhead Publishing Limited, Sawston, Cambridge, UK.

Soetaert K, Petzoldt T (2010) Inverse modelling, sensitivity and Monte Carlo Analysis in R Using Package FME. *Journal of Statistical Software,* **33**, 28.

Stasinopoulos DM, Rigby RA (2007) Generalized additive models for location scale and shape (GAMLSS) in R. *Journal of Statistical Software,* **23**, 1-46.

Stolwijk AM, Straatman H, Zielhuis GA (1999) Studying seasonality by using sine and cosine functions in regression analysis. *Journal of Epidemiology and*

Community Health, **53**, 235-238.

Stueland S, Hatai K, Skaar I (2005) Morphological and physiological characteristics of *Saprolegnia* spp. strains pathogenic to Atlantic salmon, *Salmo salar* L. *Journal of Fish Diseases,* **28**, 445-453.

Tong YL (1976) Parameter estimation in studying circadian rhythms. *Biometrics,* **32**, 85-94.

Viney ME, Riley EM, Buchanan KL (2005) Optimal immune responses: immunocompetence revisited. *Trends in Ecology and Evolution,* **20**, 665-669.

Voss Jr EW, Groberg Jr WJ, Fryer JL (1980) Metabolism of coho salmon Ig. Catabolic rate of coho salmon tetrameric Ig in serum. *Molecular Immunology,* **17**, 445-452.

Wood SN (2006) *Generalized additive models: an introduction with R,* Boca Raton, Florida, Chapman & Hall/CRC.

Ye J, Bromage ES, Kaattari SL (2010) The strength of B cell Interaction with antigen determines the degree of IgM polymerization. *The Journal of Immunology*, **184**, 844–850.

Ye J, Kaattari IM, Ma C, Kaattari S (2013) The teleost humoral immune response. *Fish and Shellfish Immunology,* **35**, 1719-1728.

Zimmerman LM, Paitz RT, Vogel LA, Bowden RM (2010) Variation in the seasonal patterns of innate and adaptive immunity in the red-eared slider (*Trachemys scripta*). *Journal of Experimental Biology,* **213**, 1477-1483.

Tables and Table legends

Parameter	Definition	Estimate	Method of estimation
x	Constant	1.28 ± 0.37	Constrained fitting of *Saprolegnia* α data to (1)
c	Immunocompetence coefficient		
a	Amplitude of immunocompetence driver		
k	c × a	2.74 ± 0.53	Constrained fitting of *Saprolegnia* α data to (1)
Θ^1	Acrophase of immunocompetence driver	1.28 ± 0.29	Constrained fitting of *Saprolegnia* α data to (1)
d	Thermal coefficient	-0.375	Intermediate value from GAMLSS models (experiments 1 and 2)
b	Amplitude of thermal driver	5.02 ± 0.27	Cosinor regression of environmental temperature (*E*) on time (*t*)
Θ^2	Acrophase of thermal driver	1.30 ± 0.05	Cosinor regression of *E* on *t*

Table 1 Parameters from sinusoid model of *Saprolegnia* α variation in experiment 3.

Gene	Model type	T (7-23°C) Parameter	T (7-23°C) *P*	Δ T (-8, 0, +8°C shift) Parameter	Δ T (-8, 0, +8°C shift) *P*
cd8a	LM	0.009±0.001	1.7×10^{-8}		
ighm	LM	0.007±0.001	5.5×10^{-11}	-0.004±0.001	4.0×10^{-5}
ighz	GAMLSS	α -0.096±0.045	0.028	α 0.012±0.050	0.009
foxp3b	LM	0.009±0.002	9.6×10^{-6}	-0.006±0.002	0.009
il4	LMM	0.0004±0.0002	0.037		
il17	LMM	-0.002±0.001	0.035		
orai1	LMM	-0.003±0.001	2.5×10^{-5}		
tirap	LM	0.009±0.001	5.7×10^{-13}		
tbk1	LMM	-0.0014±0.0002	2.8×10^{-12}		
il1r1	LMM	0.005±0.002	0.004	-0.005±0.002	0.010
lyz	LM	0.010±0.002	2.1×10^{-6}		
defbl2	LM	0.008±0.002	2.4×10^{-4}		

Table 2 Significant effects of thermal regimen on immune gene expression in experiment 1. Parameters and *P* values for prevailing temperature (T) and prior thermal shift (ΔT). T and ΔT are represented as continuous variables; no additional genes were found to be thermally-dependent through representing T and ΔT with quadratic terms. Data were analyzed in confounder-adjusted general linear models (LM), linear mixed models (LMM) and generalized additive models for location, scale and shape (GAMLSS). Genes without significant effects for T or ΔT are omitted; there were no significant T × ΔT effects. Note that for the GAMLSS model above the parameter sign is opposite to the direction of the biological effect.

Gene	Model type	T (7-15°C)		WL (0-3 months at 7°C)	
		Parameter	*P*	Parameter	term *P*
ighm	LMM			1 mo -0.012±0.006 2 mo -0.019±0.006 3 mo -0.016±0.007	0.013
il17	LM	-0.005±0.003	0.090	3 mo 0.077±0.027	0.020
il12ba	LM	0.019±0.007	0.005		
orai1	LM	-0.015±0.004	0.001		
tbk1	LMM	-0.010±0.002	9.1×10^{-6}		
il1r1	LMM			2 mo 0.014±0.007 3 mo 0.028±0.008	0.002
defbl2	LM	0.016±0.005	0.002		
gpx4a	LMM	-0.0007±0.0002	1.8×10^{-3}	1 mo 0.0035±0.0018 2 mo 0.0061±0.0019 3 mo 0.0056±0.0020	0.011

Table 3 Significant effects of thermal regimen on immune gene expression in experiment 2. Parameters and *P* values for prevailing temperature (T) and simulated prior winter length (WL). T is represented as a continuous variable (no additional genes were found to be dependent on T through adding a quadratic term); WL is represented as a factor as differences were associated with any simulated winter exposure or only with longer exposures. Data were analyzed in confounder-adjusted general linear models (LM), linear mixed models (LMM) and generalized additive models for location, scale and shape (GAMLSS). Genes without significant effects for T or WL are omitted; there were no significant T × WL effects.

Gene	Model type	Parameter (+2°C)	*P*
cd8a	LMM	0.0248±0.0122	0.042
il12ba	LM	0.0804±0.0209	1.7×10^{-4}
tbk1	LMM	-0.0713±0.0194	2.7×10^{-4}
defbl2	LMM	0.0012±0.0003	4.2×10^{-5}

Table 4 Significant effects of thermal regimen on immune gene expression in experiment 3. Parameters and *P* values for thermal treatment (unheated / +2°C). Data were analyzed in confounder-adjusted general linear models (LM), linear mixed models (LMM) and generalized additive models for location, scale and shape (GAMLSS). Genes without significant effects for thermal treatment are omitted.

Figure legends

Fig. 1 Overview of experiments (expts) 1-3, showing timeline for temperature regimens (colour blocks), experimental time points (dotted lines) and experimental readouts associated with these points (circles). In the representation of experiment 2 the timings at the end of the experiment are not shown to exact scale for simplicity (precise timings are given in the materials and methods). For *Saprolegnia* and *Gyrodactylus* challenges, the time point shown is that for initial exposure. Abbreviations: h, hours; w, weeks, mo, months. Sample sizes within cells of these experiments are given in Tables S1-S3.

Fig. 2 Manipulation of temperature in mesocosm experiment (experiment 3). (a) Temperature differential between heated and unheated tanks based on 5-minutely recording (average temperature in heated tanks – average temperature in unheated tanks). (b) Temporal thermal variation in mesocosms: scatterplot of 5-minutely temperature recording for individual tanks. Experiment days are timed from October 4th 2013.

Fig. 3 Effects of prevailing temperature and past temperature change on gene expression and disease progression in experiments. (a) Colour matrix showing significant gene expression responses to temperature regimens in experiments 1, 2 and 3 (see key). Open circles indicate responses to prevailing temperature and stars responses to previously experienced temperature change (i.e., lagged effects). As expected, the numbers of genes responding detectably to prevailing temperature fell with the thermal range examined in the respective experiments (experiment 1, 16°C range: 12/14 responsive genes; experiment 2, 8°C range: 6/14 responsive genes; experiment 3, 2°C range: 4/14 responsive genes). There was consistency across experiments in the sign of significant responses to prevailing temperature, which were always the same for a given gene (10 comparisons). Fewer genes (< half the number) responded detectably to lagged temperature effects than to prevailing temperature across experiments 1 and 2. For lagged effects shown in (a), genes are

termed cold-biased if they had higher expression than expected following a downwards temperature shift (experiment 1) or if they responded positively to increasing winter length (experiment 2). (b-e) Significant responses of *Saprolegnia* infection outcome to thermal regimen in experiments 1-3; plots (on the scale of the model linear predictor) show confounder-adjusted effects from generalized additive models for location, scale and shape (GAMLSS) with 95% confidence intervals (shaded). In experiments 1 (b) and 2 (c) the probability of not developing overt symptoms (α) decreased with increasing prevailing temperature. There was a protective residual effect of a recent +8°C temperature shift in experiment 1 (d). In experiment 3 symptom severity (μ) was subject to a time × temperature treatment (+2°C) interaction (e). (f-g) Significant responses of *Gyrodactylus* infrapopulation dynamics in experiment 2. Lower initial exposure temperature (shown on the x – axis) resulted in infections with higher (f) and later (g) abundance peaks (*peak*, highest count; *t peak*, time to reach highest count). Box-and-whisker plots show log-transformed data for individual infrapopulations (only exposure temperature was significant in statistical models). (h) Response of *Schistocephalus* parasitic index (infection weight / host weight, PI) to a +2°C manipulation across the year in experiment 3 (outside mesocosms). PI was significantly greater in hosts from heated mesocosms. Lines are confounder-adjusted effects from a general linear model (LM) with 95% intervals (shaded).

Fig. 4 Greater disease progression (following challenge infections) in winter in an outdoors seasonal environment (experiment 3). (a) For *Saprolegnia*, probability of not developing overt symptoms (α) was significantly variable in time and lowest in February; plot shows confounder-adjusted effects from a generalized additive model for location, scale and shape (GAMLSS) with 95% confidence intervals shaded (on the scale of the model predictor). (b-c) *Gyrodactylus* infrapopulations monitored through winter months (starting in November or February, compared to May or August) had higher (b) and later (c) abundance peaks (*peak*, highest count; *t peak*, time to reach highest count). Box-and-whisker plots show log-transformed data for individual infrapopulations (only exposure month was significant in statistical models).

Fig. 5 A latent immunocompetence variable, which independently correlates with seasonal expression in immunity genes, reconciles observations from laboratory and outdoors mesocosm experiments. (a) Results of an inverse model of observed variation in *Saprolegnia α* in experiment 3: α is explained via the superimposition of a sinusoidal seasonal temperature driver, TD (parameterized from observed relationships with temperature in the laboratory and from field temperature records), and a hypothetical (latent) sinusoidal immunocompetence variable, ID (parameterized by constrained fitting of *α* data to the model); *x* is a constant. (b) The association of the latent immunocompetence variable from the analysis shown in (a) with *ighm* relative expression (RE) in experiment 3; line shows confounder-adjusted effect (on the scale of the model linear predictor) from a linear mixed model (LMM) with random intercepts for month; 95% confidence interval shaded.

Fig. 6 Association between descriptors of temperature variability and mean temperature in outdoors mesocosms. (a) variance vs mean temperature; (b) maximum upward trend vs mean temperature; (c) pairwise month-to-month distances between time series shapes (Fourier coefficient distances, FCDs) vs pairwise month-to-month temperature differences; (d) amplitude of diel temperature variation vs mean temperature. Analyses shown above are based on the final 7-day period fish spent in the mesocosm habitats prior to monthly exposures to *Saprolegnia* in the 2014-2015 run of experiment 3. Panel (e) shows monthly temperature trajectories for the 7-day period analyzed, from -168 to 0 h.

Supplement

Table S1

Sample	7°C	7→15°C	15→7°C	15°C	15→23°C	23→15°C	23°C
Saprolegnia	34/2	4/9	8/14	38/22	13/6	9/15	38/16
Gene expression	19	9	14	29	20	16	21

Table showing sample sizes within the temperature treatments in experiment 1. For *Saprolegnia*, the number of fish exposed precedes the number of non-exposed control fish, separated by a slash. Numbers relate to fish entering final analyses.

Table S2

Sample	Sampling period	0 months	1 month	2 months	3 months
Gene expression	Baseline	10	-	-	-
Saprolegnia	1	1/4	3/4	4/2	2/3
Gyrodactylus	1	5	4	4	3
Gene expression	1	5	7	8	5
Saprolegnia	2	3/2	3/3	3/3	1/3
Gyrodactylus	2	5	5	3	3
Gene expression	2	5	6	6	4
Saprolegnia	3	1/3	3/2	2/2	2/2
Gyrodactylus	3	4	5	4	3
Gene expression	3	4	5	4	4
Saprolegnia	4	2/9	4/6	4/4	1/6
Gyrodactylus	4	5	9	7	4
Gene expression	4	11	10	8	7

Table showing sample sizes within the temporal thermal regimen in experiment 2 (0-3 months simulated winter × sampling period). For *Saprolegnia*, the number of fish exposed precedes the number of non-exposed control fish, separated by a slash. Sampling periods correspond to a baseline sample at the beginning of the experiment, and to times just before the warming phase of the experiment (1), during the warming phase (2-3) and after the warming phase (4). Numbers relate to fish entering final analyses.

Table S3

Sample	Cohort	Month	Ambient	+ 2°C
Gene expression	1 (2013-2014)	Oct	8	8
Gene expression		Nov	10	9
Gene expression		Dec	10	10
Gene expression		Jan	9	10
Gene expression		Feb	10	10
Gene expression		Mar	10	10
Gene expression		Apr	9	10
Gene expression		May	10	10
Gene expression		Jun	9	9
Gene expression		Jul	10	9
Gene expression		Aug	10	10
Gene expression		Sep	10	10
Gene expression	2 (2014-2015)	Dec	10	10
Saprolegnia		Dec	10/10	9/10
Gene expression		Jan	9	10
Saprolegnia		Jan	10/10	10/10
Gene expression		Feb	10	10
Saprolegnia		Feb	10/10	10/10
Gyrodactylus		Feb	19	19
Gene expression		Mar	10	10
Saprolegnia		Mar	10/10	10/10
Gene expression		Apr	10	10
Saprolegnia		Apr	10/10	10/10
Gene expression		May	10	10
Saprolegnia		May	10/6	10/6
Gyrodactylus		May	19	20
Gene expression		Jun	10	9
Saprolegnia		Jun	6/3	10/2
Gene expression		Jul	10	10
Saprolegnia		Jul	10/6	10/5
Gene expression		Aug	8	10
Saprolegnia		Aug	10/6	10/6
Gyrodactylus		Aug	9	10
Gene expression		Sep	10	10
Saprolegnia		Sep	10/7	8/1
Gene expression		Oct	10	10
Saprolegnia		Oct	10/14	10/6
Gyrodactylus		Nov	16	11

Table showing sample sizes within the temperature treatments in experiment 3, broken down by sampling time point. For *Saprolegnia*, the number of fish exposed precedes the number of non-exposed control fish, separated by a slash. Numbers relate to fish entering final analyses.

Table S4

Gene	Ensembl number (or source of sequence information)	Role
cd8a	ENSGACG00000008945	Cytotoxic T cell responses
foxp3b	ENSGACG00000012777	Regulatory T-helper cell responses
orai1	ENSGACG00000011865	T cell activation
tbk1	ENSGACG00000000607	Induced innate antimicrobial responses
il1r-like	ENSGACG00000001328	Inflammatory responses (a member of the interleukin 1 receptor genomic cluster)
ighm	ENSGACG00000012799	Antibody responses (systemic)
ighz	Gambón-Deza *et al.* (2010)	Antibody responses (secretory)
il12ba	ENSGACG00000018453	T-helper cell type 1 (Th1) responses
il17	ENSGACG00000001921	T-helper cell type 17(Th17) responses
il4	Ohtani *et al.* (2008)	T-helper cell type 2(Th2) responses
defbl2	ENSGACG00000020700	Standing and induced innate antimicrobial responses
lyz	ENSGACG00000018290	Standing and induced innate antimicrobial responses
tirap	ENSGACG00000006557	Induced innate antimicrobial responses
gpx4a	ENSGACG00000013272	Anti-oxidative activity correlated to immune activity

Table showing genes measured by quantitative real-time PCR (Q-PCR) and their role in the immune system (Hablützel *et al.* 2016).

Gambón-Deza F, Sánchez-Espinel C, Magadán-Mompó S (2010) Presence of an unique IgT on the IGH locus in three-spined stickleback fish (*Gasterosteus aculeatus*) and the very recent generation of a repertoire of VH genes. *Developmental and Comparative Immunology*, **34**, 114-122.

Hablützel IP, Brown M, Friberg IM, Jackson JA (2016) Changing expression of vertebrate immunity genes in an anthropogenic environment: a controlled experiment. *BMC Evolutionary Biology*, **16**, 1-12.

Ohtani M, Hayashi N, Hashimoto K, Nakanishi T, Dijkstra J (2008) Comprehensive clarification of two paralogous interleukin 4/13 loci in teleost fish. *Immunogenetics*, **60**, 383-397.

Appendix S1

Technical specification of mesocosm experiment (experiment 3)

For experiment 3 we used a system of mesocosms situated outside on the campus at Aberystwyth University (52.4151°, −4.0670°). The experiment was repeated twice, once in 2013-2014 and once in 2014-2015. For each experiment run we stocked the mesocosm system with a different young-of-the-year (0+) stickleback cohort collected at the end of the breeding season from an upland lake in mid Wales (52.3599°, −3.8773°). Prior to the beginning of each experiment run, lake fish destined for the mesocosms were exposed to two consecutive anthelmintic praziquantel treatments (24 h at 4 mg l^{-1}; FlukeSolve, Fish Treatment Limited), separated by four days, following manufacturer's recommendations. This removed *Gyrodactylus* spp. that might initiate epizootics detrimental to fish health. Fish were then acclimatized in the mesocosm system for 4-6 weeks. Mesocosms were filled with conditioned tap-water and routinely run at ~ 1% salinity as a prophylactic measure to supress epizootics with harmful environmental pathogens such as *Ichthyophthirius*. Mesocosms were arranged in a 3 × 4 array of 12 re-circulating 300L tanks covered with loosely fitting translucent lids and exposed to the open air. Each tank contained standardized environmental enrichment (plastic aquarium plants) and a layer of light coloured gravel. A 2 × 2 factorial combination of temperature and ration treatments was applied across the mesocosms. For the temperature treatment half of the tanks were left unheated and the remainder were heated to 2°C above the ambient temperature via 300 W shielded heaters controlled by digital differential thermostats (± 0.1°C sensitivity). For temperature control purposes, each heated tank was paired to an adjacent unheated tank, with both providing thermistor feeds to the associated digital differential thermostat. The food treatment (part of another study) involved two ration levels of the same food (chironomid larvae weekly supplemented with cladocerans). This food treatment produced similar growth trajectories with a small body weight (intercept) response of ~ +80mg in the higher ration group. The ration treatment thus involved a relatively small manipulation and a term representing its effect is considered in the statistical analyses described in the main text. For the 2013-2014 experiment run, water re-circulation was achieved through two closed systems (heated and unheated) joining 6 tanks in series in each case (recirculation in each system was at 3310 L h^{-1}via a Blagdon MDP3500 pump). For the 2014-2015 run, every tank was isolated and contained an individual stand-alone water pump and biological filter unit (Blagdon, InPond 3000; light-emitting diode spotlight disabled) with an internal 9w ultraviolet C lamp; re-circulation within individual tanks was at 1500 L h^{-1}. In 2014-2015, continuous aeration was provided by subsurface airline feeds to each tank from a Hozelock A1500 air pump (~125 L h^{-1} $tank^{-1}$). Natural plankton communities formed during the experiment that were limited, rather than ablated, by the ultraviolet irradiation included in 2014-2015. Temperature in each mesocosm tank was logged every 5-10 min, to a reading resolution ≤0.05 °C, throughout the experiment by Tinytag radio temperature loggers (TGRF-3024) networked through a Tinytag Radio system. Trials within the tank microenvironments (using a pair of calibrated Tinytag [Aquatic 2 TG-4100] data loggers placed at different stations) indicated that flow rates were sufficient to disperse temperature gradients in the vicinity of heaters and due to general environmental temperature change (at most gradients were measured at 0.5-0.6°C). Individual fish thus had very limited potential for temperature selection. Nitrite and

nitrate levels (Tropic Marin Nitrite-Nitrate test) were continuously monitored throughout the experiment and remedial water changes carried out when nitrite levels rose above 0.02 mg L^{-1}.

In the 2013-2014 and 2014-2015 runs, the mesocosm system was, respectively, initially stocked with approximately 480 and 680 acclimated fish. More fish were stocked in the second run in order to provide samples for *Saprolegnia* and *Gyrodactylus* experimental challenges at Cardiff University (see below). During acclimation prior to the experiment, mortality stabilized to a low background rate and continued to be low during the experiment runs (average monthly risk of death of ~1.5%). During the experiment, initially 40 and then 20 fish were sampled for gene expression measurements every month. At first 40 fish were sampled per month (with the aim of ultimately processing 20) to allow for technical failures, but as such failures were rare the sample taken was reduced to 20 per month. In these samples, 25% of fish were taken from each temperature × ration treatment combination and approximately equal numbers from each individual mesocosm tank (see also main text), although tank was not an important variable in statistical analyses.

Sampled fish were individually hand-netted (±2 h of 12:00 h UTC), using rapid net sweeps, and immediately killed by concussion and decerebration to prevent artefacts associated with trapping or handling. Killed fish were immediately placed in RNA stabilization solution (Hablützel *et al.* 2016) and transferred to 4°C (overnight) and then to -80°C for long-term storage.

In the 2014-2015 experiment run, as described in the main text, samples of fish were additionally extracted from the mesocosms to carry out challenge infections with *Saprolegnia* or *Gyrodactylus* at Cardiff University. Between December 2014 and October 2015 ~20-40 fish were removed for the *Saprolegnia* infections every month. Other fish were removed quarterly for *Gyrodactylus* infections (February, 40; May, 40; August, 20; November, 27). Fish were drawn in approximately equal numbers from the temperature × ration treatment combinations and as far as possible from individual mesocosm tanks (although late in the experiment run more fish were drawn from some tanks in order to equalize variation in density).

The relatively large tank sizes (300 L) allowed fish to be stocked at very low densities to negate biological crowding effects, but at the same time in sufficient abundance to undergo elective social interaction. Approximate numbers of stickleback individuals and biomass density within the mesocosms during the experiment runs are plotted and considered further in Figure S1 below.

During sampling in experiment 3 we attempted to select fish randomly, but cannot totally eliminate the possibility of bias towards the earlier capture of bolder or more weakly swimming fish. We note, however, that any such bias would be manifested as monotonic temporal trends (i.e., less surviving poor swimmers, or bold individuals). The trends we focus on in the main article (seasonally-biased disease progression and immmunocompetence) are, in contrast, convex associations with time and thus unlikely to be artefacts of an ease-of-capture bias.

Hablützel IP, Brown M, Friberg IM, Jackson JA (2016) Changing expression of vertebrate immunity genes in an anthropogenic environment: a controlled experiment. *BMC Evolutionary Biology*, **16**, 1-12.

Figure S1

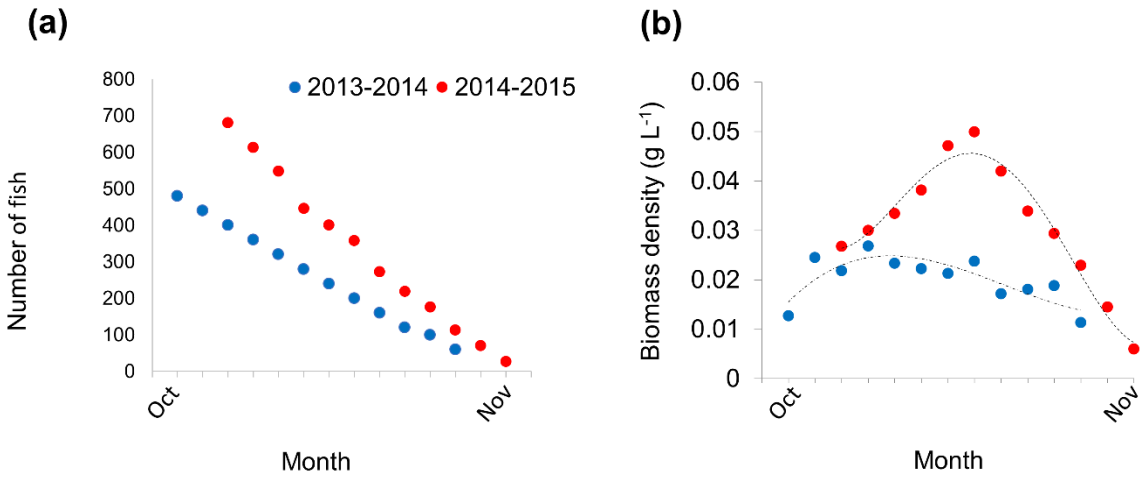

Plots showing total numbers of individuals (a) and biomass density (b) of sticklebacks in each run of the mesocosm experiment (experiment 3). We note that progressive decrease in the number of individuals (primarily due to sampling) was compensated by increasing biomass, so that biomass density was maintained within narrow absolute margins of variation (~ 0.01-0.05 g L^{-1}) and at relatively very low levels. Although the different sampling schedules in different year runs produced different temporal patterns in biomass density, the pattern for 2014-2015 does not correspond to the timing of the latent anti-*Saprolegnia* immunocompetence variable derived (for 2014-2015) in the main text. Thus, biomass density peaked during April/May, whilst the latent immunocompetence variable peaked during July/August (half out of phase)

Figure S2

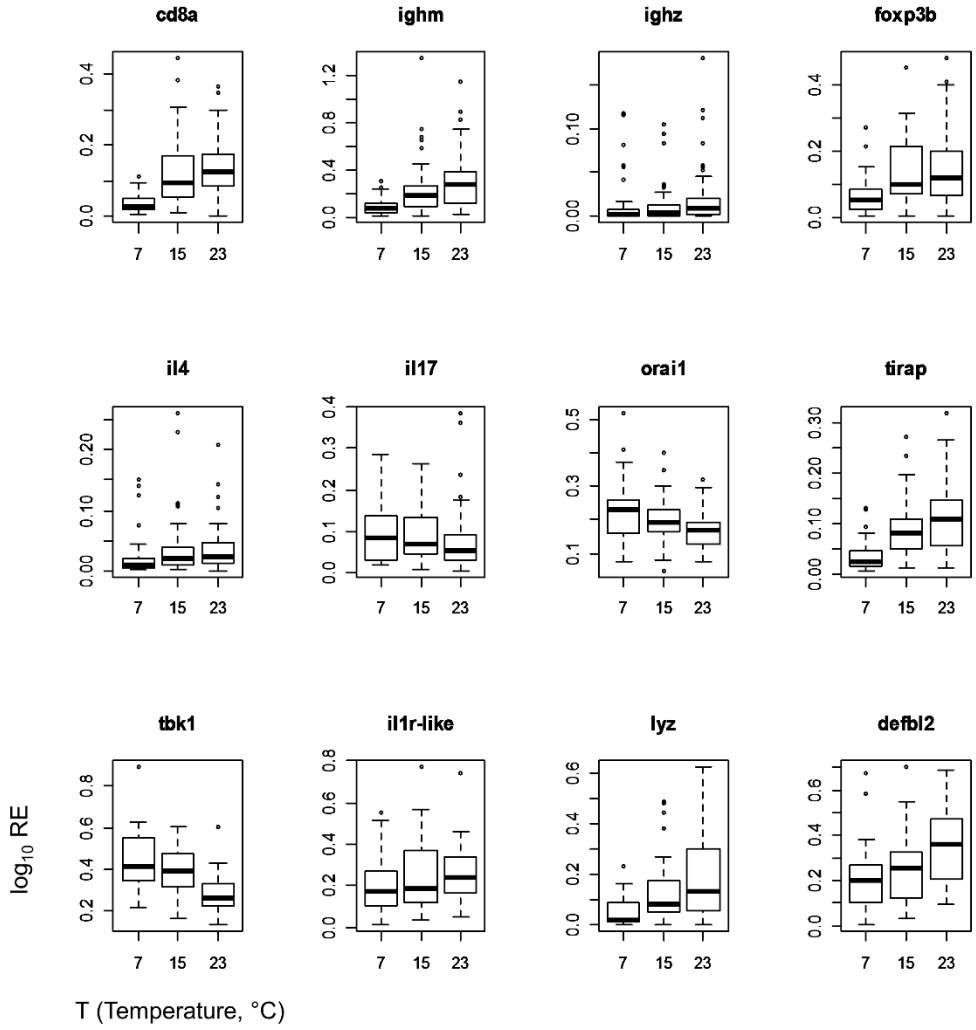

Box-and-whisker plots of $\log_{10}(x+1)$ transformed gene relative expression (RE) data from experiment 1 with respect to prevailing temperature (T). Data shown only where there was a significant effect of T in statistical models.

Figure S3

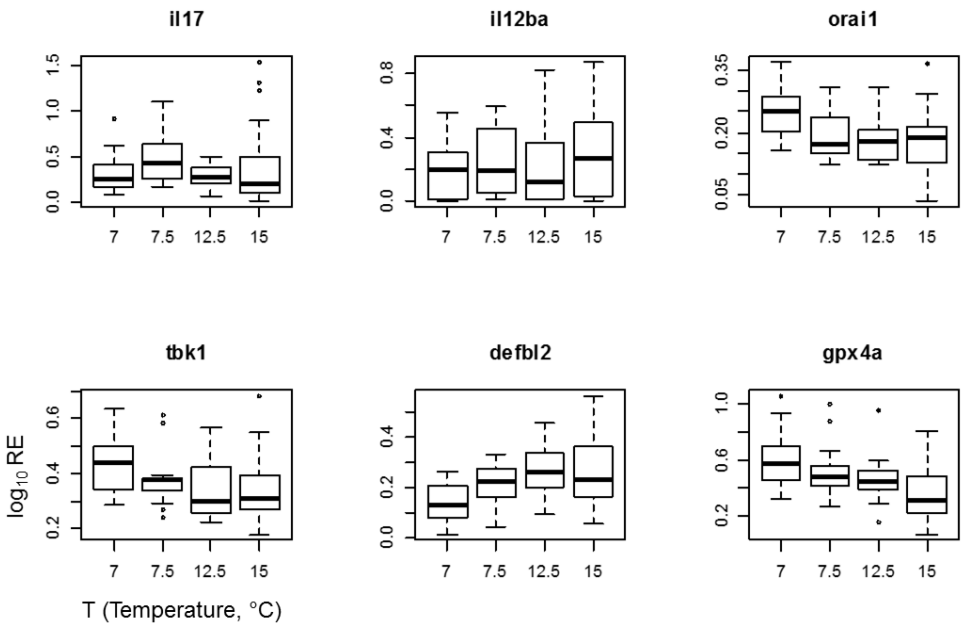

Box-and-whisker plots of $\log_{10}(x+1)$ transformed gene relative expression (RE) data from experiment 2 with respect to prevailing temperature (T). Data shown only where there was a significant effect of T in statistical models.

Figure S4

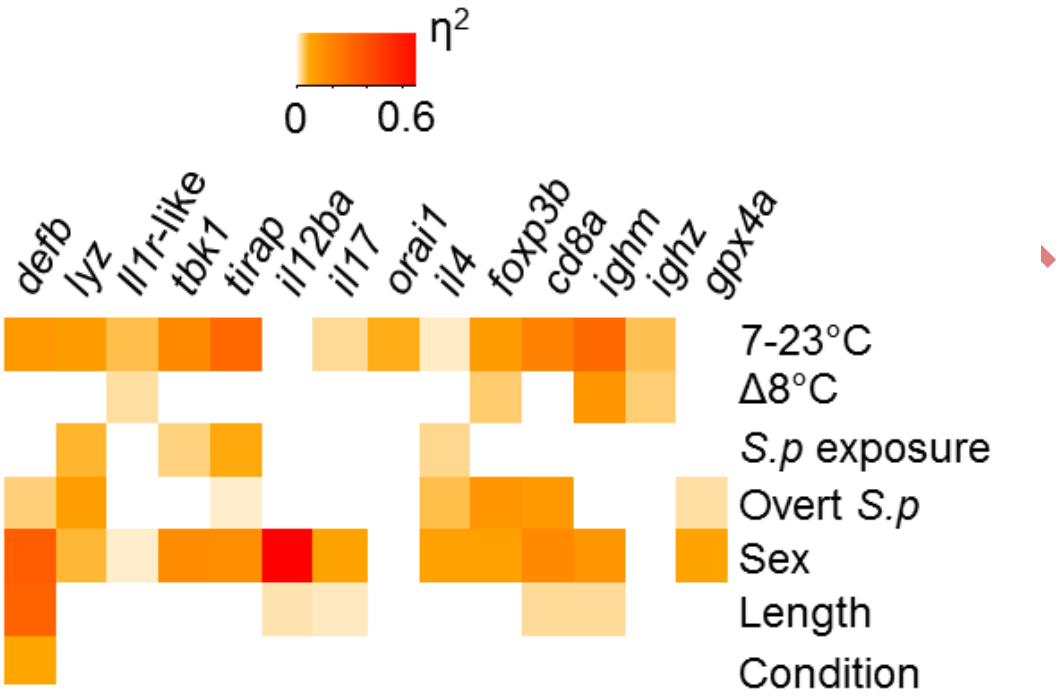

Heat plot of effect size (partial eta squared, η^2) for variables in experiment 1 (all results are from general linear models for comparability); where a term is absent from the minimally adequate model this is indicated as an uncoloured tile. S.p., *Saprolegnia parasitica*. Overt S.p., presence or absence of overt *S. parasitica* symptoms.